

# *Morphology, phylogeny, and toxicity of Atama complex (Dinophyceae) from the Chukchi Sea*

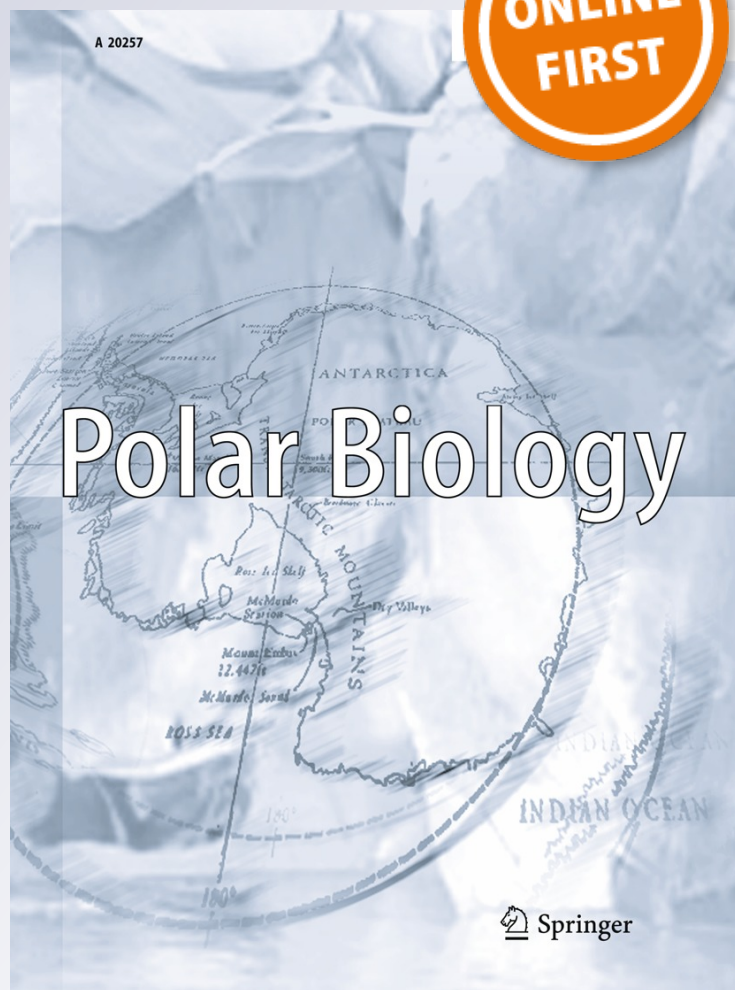
**Haifeng Gu, Ni Zeng, Zhangxian Xie,  
Dazhi Wang, Weiguo Wang & Weidong  
Yang**

**Polar Biology**

ISSN 0722-4060

Polar Biol

DOI 10.1007/s00300-012-1273-5



**Your article is protected by copyright and all rights are held exclusively by Springer-Verlag Berlin Heidelberg. This e-offprint is for personal use only and shall not be self-archived in electronic repositories. If you wish to self-archive your work, please use the accepted author's version for posting to your own website or your institution's repository. You may further deposit the accepted author's version on a funder's repository at a funder's request, provided it is not made publicly available until 12 months after publication.**

# Morphology, phylogeny, and toxicity of *Atama* complex (Dinophyceae) from the Chukchi Sea

Haifeng Gu · Ni Zeng · Zhangxian Xie ·  
Dazhi Wang · Weiguo Wang · Weidong Yang

Received: 4 August 2012 / Revised: 20 November 2012 / Accepted: 21 November 2012  
© Springer-Verlag Berlin Heidelberg 2012

**Abstract** The “Atama complex”, which consists of *Alexandrium tamarense*, *A. fundyense*, and *A. catenella*, is one of the most important groups within the dinoflagellate genus *Alexandrium*. Information of the biogeography of the Atama complex is limited in the Arctic Ocean. In the present study, we established 55 strains of the Atama complex by incubating ellipsoidal cysts collected from the Chukchi Sea. The vegetative cells are characterized by a prominent ventral pore, thereby fitting the description of *A. tamarense* morphotype. Large subunit (LSU) and/or internal transcribed spacer (ITS) region sequences of these strains were examined. Both sequences showed intragenomic polymorphism. The 708 bp of the LSU sequences from the strains differed from each other at 0–44 sites (0.0–6.2 %), and the ITS region sequences differed from one another at 0–28 sites (0.0–5.4 %). Phylogenetic analysis revealed that the Chukchi Sea strains were nested within Atama complex (Group I). Assessment of paralytic shellfish poisoning toxin production by four Chukchi Sea

strains using high-performance liquid chromatography showed that total toxin per cell ranged from 9 to 41 fmol cell<sup>-1</sup>. The toxin profile of the four strains from the Chukchi Sea is conserved, with the major toxins being *N*-sulfocarbamoyl toxin (C2), saxitoxin, and gonyautoxin-4. Our results support that dispersal of the Atama complex (Group I) from the Bering Sea to the Chukchi Sea might have occurred.

**Keywords** *Alexandrium tamarense* · Atama complex · Chukchi Sea · Morphology · Phylogeny · PSP toxin

## Introduction

The “Atama complex”, one of the most important groups within the dinoflagellate genus *Alexandrium*, refers to three morphospecies: *A. tamarense* (Lebour) Balech, *A. fundyense* Balech, and *A. catenella* (Whedon and Kofoid) Balech. Presence/absence of a ventral pore in the first apical plate is the key morphological feature differentiating these species. *A. tamarense* always has a ventral pore, whereas *A. catenella* and *A. fundyense* lack such a pore. Another important characteristic that differentiates these species is the ability to form chains: *A. catenella* can form long cell chains, whereas *A. fundyense* is always solitary. The Atama complex can produce paralytic shellfish poisoning (PSP) toxin, and the toxin profile of the Atama complex has been considered to be regionally conserved (Cembella 1998). In addition, the Atama complex forms massive harmful blooms worldwide, which are responsible for serious ecological and economic losses (Kim et al. 2002; Weise et al. 2002; Genovesi et al. 2009; Aguilera-Belmonte et al. 2011; Crespo et al. 2011; Anderson et al. 2012).

**Electronic supplementary material** The online version of this article (doi:10.1007/s00300-012-1273-5) contains supplementary material, which is available to authorized users.

H. Gu (✉) · N. Zeng · W. Wang  
Third Institute of Oceanography, SOA,  
Xiamen 361005, China  
e-mail: haifenggu@yahoo.com

Z. Xie · D. Wang (✉)  
State Key Laboratory of Marine Environmental Science,  
Environmental Science Research Center, Xiamen University,  
Xiamen 361005, China  
e-mail: dzwang@xmu.edu.cn

W. Yang  
College of Life Science and Technology, Jinan University,  
Guangzhou 510632, China

Lilly et al. (2007) recommended that use of the morphospecies appellations within this complex be discontinued as they imply erroneous relationships among morphological variants. These authors subdivided the Atama complex into five groups (Group I to V) using large subunit (LSU) sequence-based phylogeny. Recently, Miranda et al. (2012) analyzed the small subunit ribosomal rRNA gene (SSU rDNA) of the Atama complex and established two well-separated clades: strains with high intragenomic polymorphism (IRP) sequences were grouped in Clade I (High-IRP clade = Group I), and strains without or with low-IRP sequences were grouped in Clade II (No/Low-IRP clade = Groups II–IV). According to Miranda et al. (2012), Clade I is likely to constitute a species as postulated, while Clade II contains other one or more species, with the several subclades unable to be partitioned to proper taxonomic units due to insufficiency of data. The reproductive barrier between Group I and Group III ribotypes suggests that they are different biological species (Brosnahan et al. 2010), which is consistent with the SSU-based conclusion (Miranda et al. 2012).

Some researchers proposed that human-assisted dispersal was responsible for the sympatric occurrence of the Atama complex of various ribotypes (Scholin et al. 1994; Lilly et al. 2002; Penna et al. 2005; Bolch and De Salas 2007). In contrast, John et al. (2003) suggested that the distribution of various Atama complex ribotypes represented a vicariant event. Natural dispersal of Atama complex (Group I) between the Pacific and the North Atlantic via the Arctic Ocean was hypothesized (Scholin et al. 1995; Medlin et al. 1998). However, this hypothesis remains to be tested, as genetic information about the Atama complex in the Arctic Ocean is limited (Baggesen et al. in press), although both cells and cysts are widely distributed in the Arctic (e.g., the Beaufort Sea, the East

Siberia Sea, the Barents Sea, the west coast of Greenland) (Marret and Zonneveld 2003; Ratkova and Wassmann 2005; Niemi et al. 2011; Poulin et al. 2011) and the sub-Arctic region (e.g., the Bering Sea, Faeroe Island, the Icelandic coast, the Norwegian Sea) (Moestrup and Hansen 1988; Marret and Zonneveld 2003; Orlova et al. 2007; Burrell et al. 2012).

LSU IRP previously was reported in Atama complex (Group I) (Scholin et al. 1994; Medlin et al. 1998; Kim et al. 2004; Orr et al. 2011), but it has not been fully examined yet. Herein, we sequenced partial LSU and internal transcribed spacer (ITS) region sequences of the Atama complex collected from the Chukchi Sea. We compared these sequences with those of the Atama complex from other locales and carried out phylogenetic analysis based on both LSU and ITS sequences. Toxin profiles of four selected strains also were determined.

## Materials and methods

### Sample collection and treatment

Surface sediment samples were collected from the Chukchi Sea (Fig. 1, geographical coordinates and sample dates of the sites, see Table 1) using a grab sampler in July 2010. The samples were stored in the dark at 4 °C until further treatment. Approximately 2 cm<sup>-3</sup> of wet sediment was mixed with 20 ml of filtered seawater and sonicated for 2 min (100 W) to dislodge detrital particles. The sample was then filtered through a 100- $\mu$ m sieve and subsequently through a 20- $\mu$ m sieve. The 20–100  $\mu$ m fraction was re-suspended in 1 ml filtered seawater, and single cysts were isolated from this material by means of drawn-out Pasteur pipettes and several washing steps through droplets

**Fig. 1** Map of sampling locations in the Chukchi Sea

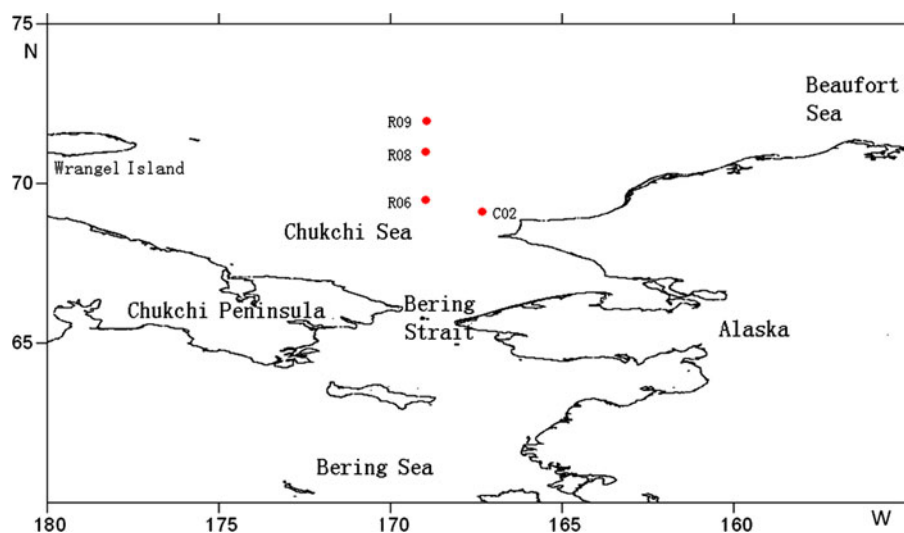


**Table 1** Location of sampling stations, their collection data, water depth, and cyst density of Atama complex

Stations	Longitude (W)	Latitude (N)	Depth (m)	Collection date	Cyst density (ind cm <sup>-3</sup> )
C02	167°20.15'	69°07.40'	49	July 21, 2010	3.2
R06	168°59.00'	69°30.00'	52	July 21, 2010	16.8
R08	168°58.81'	71°00.19'	44	July 22, 2010	19.2
R09	168°56.40'	71°57.80'	51	July 24, 2010	10.0

of sterile seawater. Cultures established by incubating single cysts were maintained in *f/2-Si* medium (Guillard and Ryther 1962) at 15 °C, 90 μmol photons m<sup>-2</sup> s<sup>-1</sup> under a 12:12 h L: D cycle (hereafter called “standard conditions”). Preliminary results showed that Atama complex from the Chukchi Sea grew faster at 15 °C than 9 °C. It took approximately 3 weeks for a single cyst to germinate and grow into a culture with cell concentration of around 1,000 cells ml<sup>-1</sup> under standard conditions.

#### Light microscopy (LM)

Vegetative cells were examined under a Zeiss Axio Imager microscope (Carl Zeiss, Göttingen, Germany) equipped with epifluorescence. Light micrographs were obtained using a Zeiss AxioCam HRC digital camera. Calcofluor white was used to discern plates in vegetative cells following the method previously described (Fritz and Triemer 1985).

#### Molecular analysis

Single cells were isolated and lysed by freezing in liquid N<sub>2</sub> overnight before PCR amplification. Partial D1–D2 of LSU rDNA and ITS regions of the 5.8S rDNA gene were amplified using primers D1R and D2C (Scholin et al. 1994) and primers ITSA and ITSB (Adachi et al. 1996).

The PCR protocol was as follows: initial denaturation for 3.5 min at 94 °C, followed by 35 cycles of 50 s denaturation at 94 °C, 50 s annealing at 45 °C, and 80 s extension at 72 °C, plus a final extension of 10 min at 72 °C. PCR products were purified using a purification kit (Lulong, Xiamen, China) and cloned into a pUCm-T vector and sequenced (1–14 clones for each strain) using the ABI Big-Dye dye-terminator technique (Applied Biosystems, Foster city, USA), according to the manufacturer's recommendation. 33 LSU sequences from 14 strains and 16 ITS sequences from six strains of Atama complex of the Chukchi Sea were selected for phylogenetic analyses

(Table S1). They were aligned with LSU rDNA and ITS sequences of the Atama complex and that of outgroup taxa available in GenBank (Tables S2, S3) using ‘MUSCLE’ (Edgar 2004) (<http://www.ebi.ac.uk/Tools/msa/muscle/>) with the default settings.

#### Phylogenetic analysis

For maximum-likelihood (ML) analysis, we used the program JModeltest (Posada 2008) to select the most appropriate model of molecular evolution with Akaike information criterion (AIC). This test chose the general time-reversible (GTR) model of substitution (Rodriguez et al. 1990) following a gamma distribution shape parameter (GTR+G). ML trees were constructed in MEGA 5.05 (Tamura et al. 2011). The robustness of tree topology was conducted using bootstrap with 1,000 replications.

A Bayesian reconstruction of the data matrix was performed with MrBayes 3.1.2 (Ronquist and Huelsenbeck 2003) using the best-fitting substitution model (GTR+G). Four Markov chain Monte Carlo (MCMC) chains ran for ten million generations, sampling every 10,000 generations. A majority rule consensus tree was created in order to examine the posterior probabilities of each clade.

#### Toxicity

For PSP toxin, aliquots of 100 ml culture at mid-exponential growth phase were collected by centrifugation at 2,500g for 5 min, followed by subsequent re-suspension in 0.5 ml of 50 mM acetic acid, and then followed by homogenization (13 W) with three successive sonication cycles (1.5 min/cycle) on ice. Approximately 20 ml of the supernatant obtained after centrifugation at 10,000g for 30 min was subjected to toxin analysis using HPLC, following the method described previously (Wang and Hsieh 2001).

## Results

#### Morphology

Atama complex cysts are dominant in surface sediments from the Chukchi Sea. The cysts are ellipsoid, 45–60 μm long, and 28–35 μm wide, and they have a bright accumulation body inside (Fig. 2a). Cyst density at the four sampling stations ranged from 3.2 to 19.2 ind cm<sup>-3</sup> (Table 1). A total of 120 cysts were isolated and incubated under standard conditions. Excystment generally took 3–5 days, and the germination rate was 65.8 %.

Fifty-five strains of Atama complex were established and their morphology was examined under light microscopy (LM). Solitary cells and chains of 2–4 cells were observed in

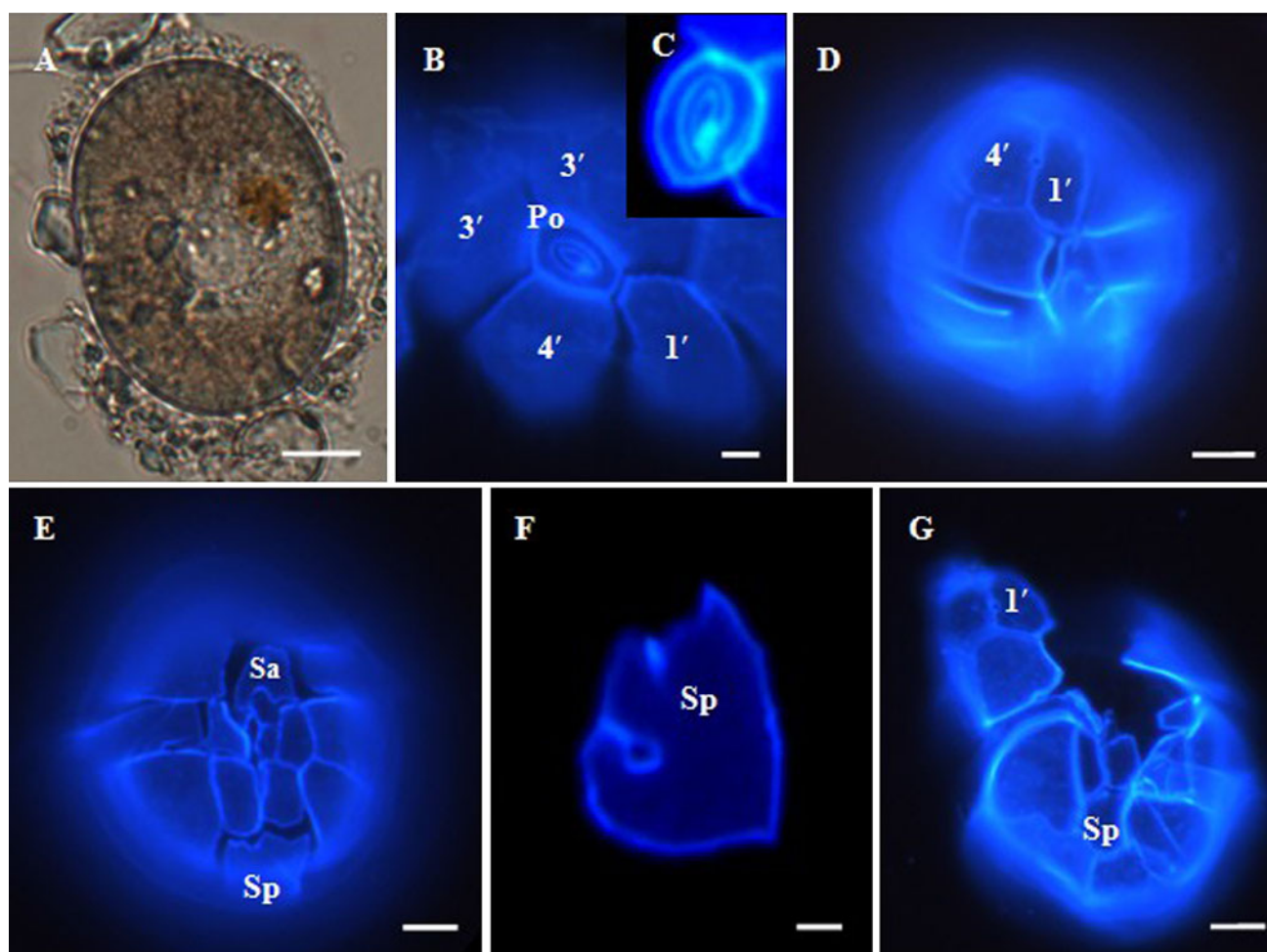


**Fig. 2** Light microscopy of vegetative cells and cysts of *Atama* complex. A living cyst of *Atama* complex collected from the Chukchi Sea showing a bright accumulation body (a); Calcofluor-stained cell in apical view (strain ATBJ41) showing the apical pore complex with a wide dorsal portion (b); Calcofluor-stained cell in apical view (strain ATBJ41) showing the apical pore complex with an irregularly oval shape (c); Calcofluor-stained cell in ventral view (strain

ATBJ41) showing a ventral pore at the junction of 1' and 4' (d); Calcofluor-stained cell in ventral view (strain ATBJ50) showing the sulcal plates (E); Calcofluor-stained posterior sulcal plate (Sp) (strain ATBJ54) showing an oval posterior attachment pore (pap) dislocated toward the right anterior margin of the Sp plate (f); Calcofluor-stained cell in ventral view (strain ATBJ54) showing the posterior sulcal plate (Sp) lacking a pap (g). Scale bars: a 10  $\mu$ m; b–e, g 5  $\mu$ m; f 1  $\mu$ m

all strains. The single cells were 30–40  $\mu$ m long and 30–38  $\mu$ m wide and from round to ovoid. Cells showed the plate formula of po, 4', 6'', 6C, 8S, 5''', 2'''''. The apical pore plate (po) varied from a wide dorsal portion to an irregularly oval shape (Fig. 2b, c). The first apical plate (1') was symmetrically rhomboidal and was directly connected with the po. A ventral pore at the suture between the 1' and 4' was always present (Fig. 2d). The anterior sulcal plate (Sa) was narrow, slightly longer than wide, and had a deep posterior sinus (Fig. 2e). The posterior sulcal plate (Sp) was rhomboidal and slightly longer than wide. A round or oval posterior attachment pore (pap) was dislocated toward the right anterior margin of the Sp plate (Fig. 2f). The posterior attachment pore was not observed in some cells (Fig. 2g).

#### Molecular analysis

Fifty-five strains of *Atama* complex from the Chukchi Sea were analyzed for LSU and/or ITS sequences. Sequences were deposited in the GenBank with accession numbers from KC019250 to KC019298 and KC113502 (Table S1). PCR amplification always yielded a single band that was approximately 700 (LSU) or 600 (ITS) bp long. IRP of LSU and ITS is generally formed by substitutions and located at random. The 708 bp of the LSU sequences differed from one another at 0–44 sites (0.0–6.2%), and the ITS region sequences differed with one another at 0–28 sites (0.0–5.4%). Two distinct genes (A and B gene) could be identified for most strains through sequencing of a few clones.

ATBJ25 that were sequenced differed from each other at 41 positions in LSU sequences. The ATBJ25 clone D (A gene, GenBank accession number: KC019253) differs from Danish strain K-0055 (GenBank accession number: AF200668) at only one position out of 708 bp, from Japanese strain HAT4 and North American strain CCMP1719 (GenBank accession numbers: AB088279, JF521624) at two positions, and from Chilean strain SD01, South African strain CTCC5 at three positions (GenBank accession numbers: HQ997921, AY311594). The ATBJ25 clone B (B gene, GenBank accession number: KC019251) differs from English strain UW4-1, Norwegian strain IMR\_S\_182008, and North American strain CCMP1719 (GenBank accession numbers: AJ303447, JF521647, JF521642) at 9, 30, and 34 positions, respectively.

Eleven ITS clones of strain ATBJ25 were sequenced and they differ from each other at 22 positions. The ATBJ25 clone A (A gene, GenBank accession number: KC019283) differs from Japanese strain FK-788 (GenBank accession number: AB006993) at only one position, and from Argentine strain MDQ1096, Norwegian strain IMR\_S\_182008, North American strain CCMP1719, English strain 04-197-A1, and Chilean strain PFB38 (GenBank accession numbers: AM292306, JF521629, JF521624, FJ042687, HM641245) at only two positions; Strain ATBJ25 clone B (B gene, GenBank accession number: KC019284) differs from Japanese strain FK-788 (GenBank accession numbers: AB006994) at only one position and from Norwegian strain IMR\_S\_182008 and North American strain CCMP1719 (GenBank accession numbers: JF521647, JF521642) at four and five positions, respectively.

### Phylogeny

The ML and BI analyses based on LSU sequences generated two similar phylogenetic trees, differing from each other only at a few topologies (Fig. 3). The Atama complex was subdivided into five well-resolved groups, i.e., Group I, II, III, IV, and V. Strains from the Chukchi Sea were all nested within the Atama complex Group I, which also incorporate strains from USA, Canada, Norway, UK, Korea, Japan, Chile, and South Africa. The polymorphic sequences from the same strain did not cluster together; they were generally distributed in several different clusters throughout the group. For instance, IRP copies from strain G25 were distributed in 4 different clusters. Two rDNA gene copies, i.e., the A gene and B gene were identified in six strains from the Chukchi Sea (Orr et al. 2011).

The ML and BI analyses based on ITS sequences generated two similar phylogenetic trees, differing from each other only at a few topologies (Fig. 4). The Atama complex was also subdivided into five well-resolved groups,

corresponding to those based on LSU sequences. Strains from the Chukchi Sea were all nested within the Atama complex Group I. The polymorphic sequences from the same strain intermingle with other strains. Two rDNA gene copies, i.e., the A gene and B gene were identified in five strains from the Chukchi Sea. A possible A-B chimera was detected in one sequence of strain ATBJ61.

### Toxicity

Six PSP toxins were identified among the four strains of Atama complex (Group I) from the Chukchi Sea: saxitoxin (STX), neosaxitoxin (neoSTX), gonyautoxin (GTX2, GTX3, GTX4), and *N*-sulfocarbamoyl toxin (C2). C1, GTX1, and GTX5 (B1) also were examined but appeared not detected. C2 was the dominant toxin, representing 31–52 % of the total toxin content on an average mole percentage basis. STX was the second most dominant toxin (13–34 %), followed by GTX3 (10–20 %) (Fig. 5). The total amount of toxin per cell ranged from 9 to 41 fmol cell<sup>-1</sup>.

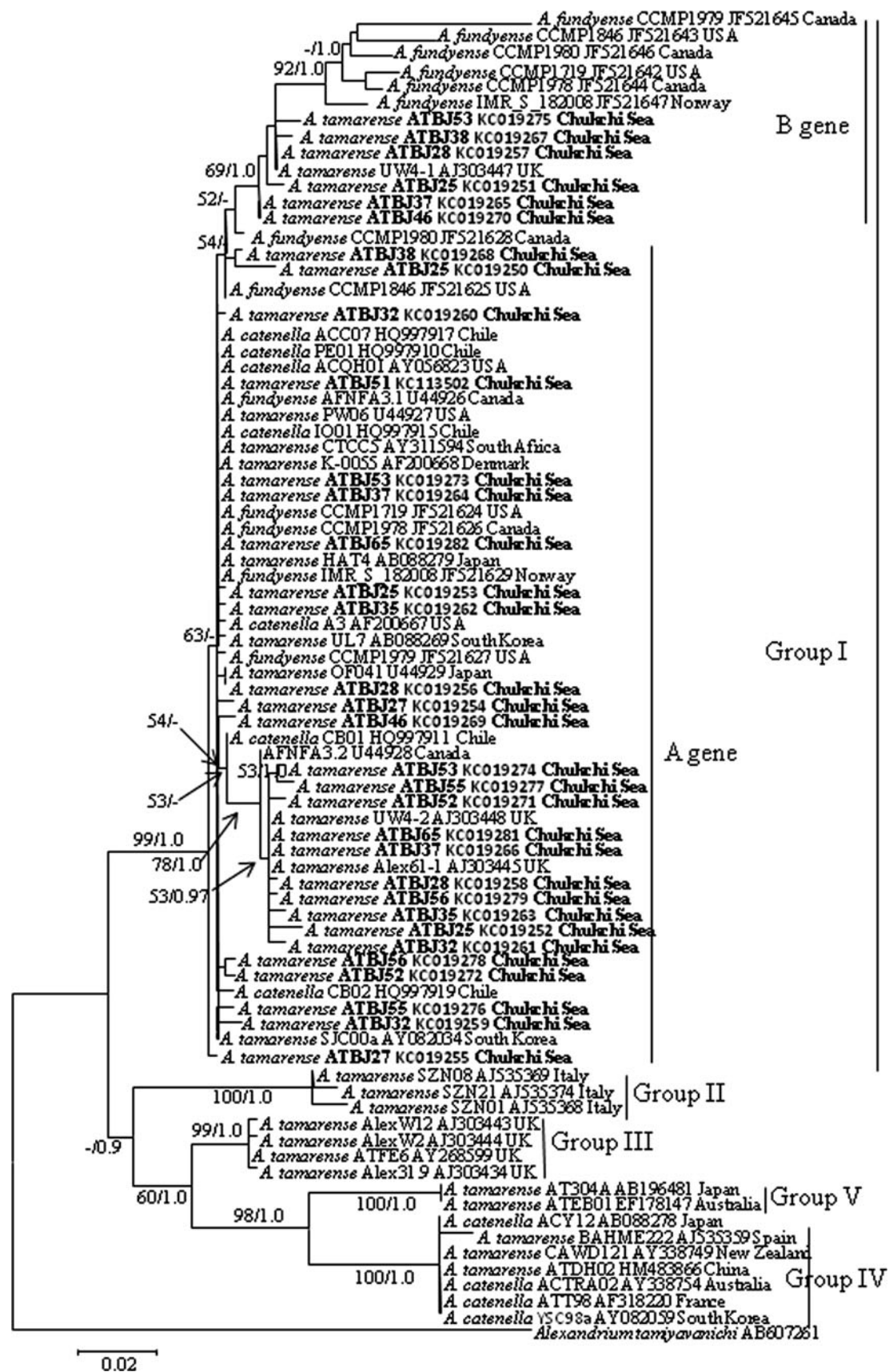
## Discussion

### Cyst distribution

Atama complex cyst density in the four sediment samples collected from the Chukchi Sea was relatively low (maximum: 19 ind cm<sup>-3</sup>) compared with that in the Gulf of Maine (maximum: 2 × 10<sup>7</sup> ind cm<sup>-3</sup>) (Anderson et al. 2005). More sediment samples from deeper stations need to be examined, as a patchy distribution of these cysts has been reported (Anderson et al. 2005). The germination rate of Atama complex cysts in the Chukchi Sea (~66 %) is comparable to that of Atama complex (as *A. fundyense*) from Gulf of Maine (>70 %) (Anderson et al. 2005).

### Molecular analysis and phylogeny

Typically, several hundred copies of the ribosomal RNA locus are present in tandem in the nuclear genome (Coleman 2007). Sequence variability among these copies can be homogenized through “concerted evolution” (Ganley and Kobayashi 2007). However, IRP is still common in some dinoflagellate species (Gribble and Anderson 2007; Thornhill et al. 2007), and diatoms as well (Alverson and Kolnick 2005). SSU IRP has been reported extensively in Atama complex (Group I) (Scholin et al. 1993; Kim et al. 2004; Miranda et al. 2012). However, not until recently (Miranda et al. 2012) has IRP information be used in concert with phylogeny to unify some of the observed variable sequences to a coherent taxonomic group



◀ **Fig. 3** Phylogeny of the Atama complex inferred from partial LSU rDNA sequences based on maximum-likelihood (ML) and Bayesian inference (BI) analyses. *Alexandrium tamiyavanichi* was used as an outgroup. Branch lengths are drawn to scale, with the *scale bar* indicating the number of nt substitutions per site. Numbers on branches are statistical support values for the clusters to the *right* of them (*left* ML bootstrap support values; *right* Bayesian posterior probabilities). Bootstrap values <50 % and posterior probabilities <0.7 are not shown

(species). Our results demonstrated that the size of LSU rDNA IRP can reach 6.5 %, which is even greater than that of SSU rDNA IRP (Miranda et al. 2012). Unlike in Atama complex (Group I) strains from the Northern Hemisphere, IRP was not reported in strains from Chile, Brazil, and South Africa (Sebastián et al. 2005; Persich et al. 2006; Varela et al. 2012). IRP in these strains might have been neglected as the Chilean strain ACC01 did show SSU IRP (Miranda et al. 2012).

#### Distribution and dispersal

The Atama complex (Group I) is restricted to areas of high latitude (above 30°) in both hemispheres (Persich et al. 2006; Lilly et al. 2007; Collins et al. 2009; Varela et al. 2012). The presence of Atama complex (Group I) strains in the Chukchi Sea supports that they are cold water species. These cells grew slowly at low temperature (4 °C), and the growth rate increased when temperature rose to 9 °C (Gu unpublished results). The sea surface temperature at our sampling stations can reach around 8–10 °C in summer (Tang et al. 2001; Woodgate et al. 2005) and thus permit their fast growth.

To date, Atama complex (Group I) strains from North Asia and Europe inevitably have a ventral pore (Medlin et al. 1998; Kim et al. 2004; Lilly et al. 2007; Collins et al. 2009), whereas those in South Africa and Chile always lack such a pore (Sebastián et al. 2005; Varela et al. 2012). Atama complex (Group I) strains from the two hemispheres might originate from the same ancestor (John et al. 2003) and evolved into a morphologically different species.

On the other hand, the high similarity among ITS rDNA sequences of Atama complex (Group I) strains worldwide suggests that this is a recently diverged species. The biogeography of this species might be due to human-assisted dispersal (Bolch and De Salas 2007) or to natural dispersal between the two hemispheres during a period when the global oceans were cooler. Natural transport during the last glacial maximum (LGM) has been proposed as an explanation for the bipolar distribution of the dinoflagellate *Polarella glacialis* and the seaweed *Acrosiphonia arcta* (Oppen et al. 1994; Montresor et al. 2003). LGM refers to a period in the Earth's climate history when ice sheets were at their maximum extension (between 26,500 and 19,000 years ago) (Clark et al. 2009). It is estimated that

Earth as a whole cooled  $3.0 \pm 0.6$  °C during that period (Hoffert and Covey 1992). During the LGM, Atama complex (Group I) strains from the two hemispheres might have been much closer geographically than at the present time, which could have facilitated dispersal between the two hemispheres.

Our finding of Atama complex (Group I) stains in the Chukchi Sea supports the premise that natural dispersal between the Atlantic and Pacific via the Arctic Ocean is feasible (Scholin et al. 1995; Medlin et al. 1998). The Bering and Chukchi seas connect through Bering Strait, which is about 85 km wide and 50 m deep. Current observations from Bering Strait showed that the flow is always northward (Coachman and Aagaard 1966), supporting that dispersal of Atama complex (Group I) from the Bering Sea to the Chukchi Sea might have occurred.

A strain of Atama complex (Group I) (as *A. fundyense*) was reported in the Norwegian Sea recently (Orr et al. 2011), although whether it was transported through human-assisted dispersal or natural dispersal remains to be determined. More strains of Atama complex from the Arctic Ocean need to be examined in the future.

#### Toxicity

Atama complex (Group I) strains from the Chukchi Sea produce STX, neoSTX, GTX2, GTX3, GTX4, and C2, which is generally consistent with findings in Atama complex (Group I) strains from USA, UK, and Chile (Anderson et al. 1994; Collins et al. 2009; Varela et al. 2012). However, our strains differ from those of Chile in producing higher proportion of STX and absence of GTX5 (Varela et al. 2012), from those of UK by absence of C1, GTX1, and GTX5 (Collins et al. 2009). Our strains also differ from those of the Bering Sea by the absence of GTX5 and relatively high levels of STX (Orlova et al. 2007). Toxin profiles have been used to differentiate populations of Atama complex (Group I) strains from the northeastern United States and Canada (Anderson et al. 1994). However, toxin content and composition can be variable in culture as a response to nutrient availability (Macintyre et al. 1997; Murata et al. 2012), and comparison between PSP-toxin profiles and genotypic characters failed to yield close associations (Alpermann et al. 2010). Whether strains from the Chukchi Sea and Bering Sea are genetically different remain to be determined.

#### Conclusions

This study describes the first observations regarding the presence and identification of Atama complex (Group I) strains from the Chukchi Sea. More strains of Atama

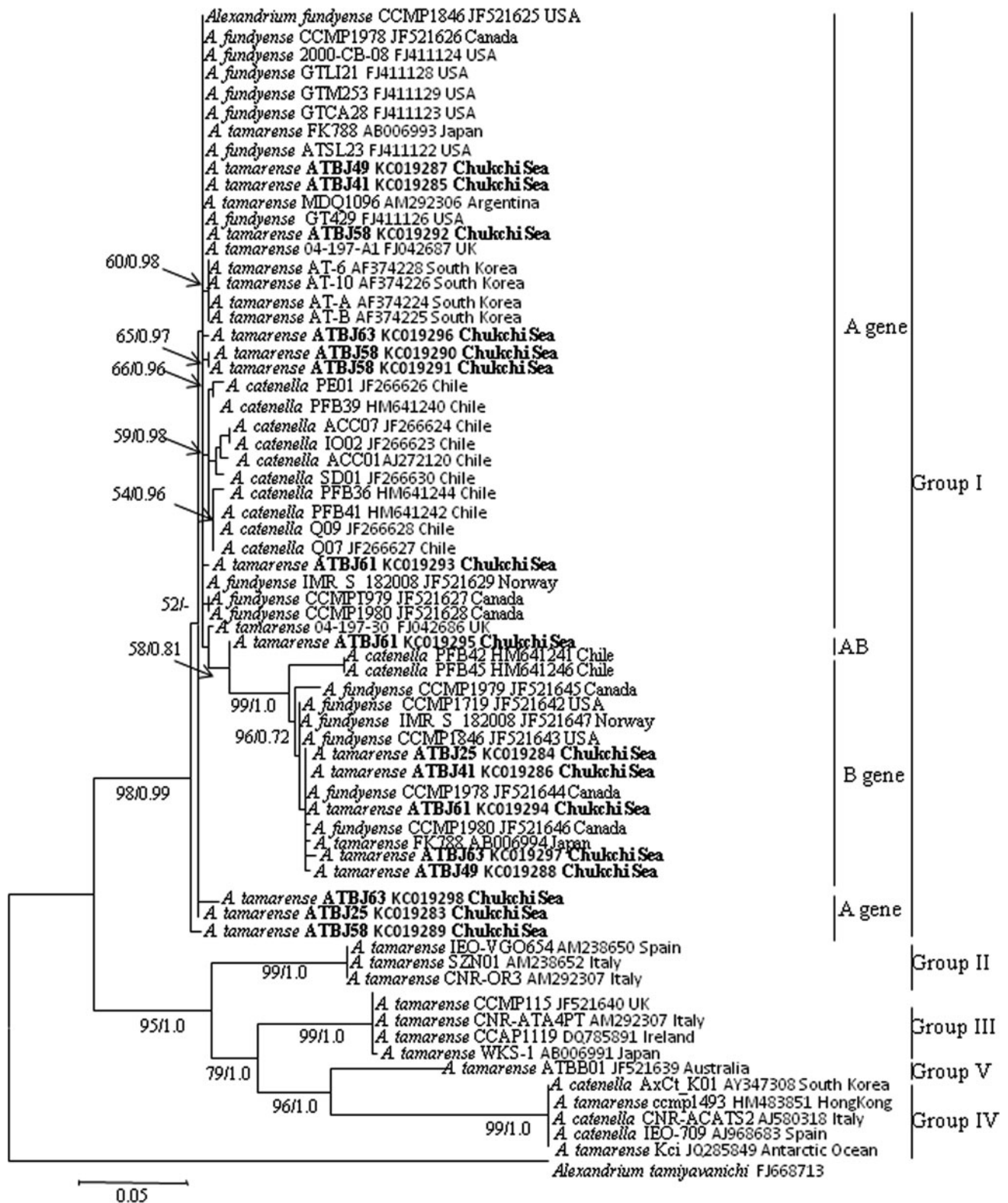


**Fig. 4** Phylogeny of the Atama complex inferred from ITS sequences based on maximum-likelihood (ML) and Bayesian inference (BI) analyses. *Alexandrium tamiyavanichi* was used as an outgroup. Branch lengths are drawn to scale, with the scale bar indicating the number of nt substitutions per site. Numbers on branches are

statistical support values for the clusters to the right of them (left ML bootstrap support values; right Bayesian posterior probabilities). Bootstrap values <50 % and posterior probabilities <0.7 are not shown

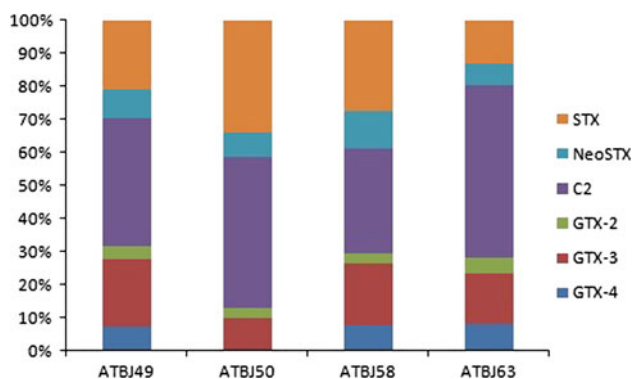


**Fig. 5** Histograms showing the PSP toxin composition (% molar) of four Atama complex (Group I) strains (ATBJ49, ATBJ50, ATBJ58, ATBJ63) established by incubating resting cysts isolated from sediments collected from the Chukchi Sea

complex from the Arctic Ocean need to be established and examined in the future, which could help to explain the current biogeography of Atama complex around the world.

**Acknowledgments** We thank Dieter Piepenburg and three anonymous reviewers for constructive suggestions to improve the manuscript. This work was supported by the China Program for International Polar Year 2007–2011, the Special Research Foundation for Public Welfare Marine Program (201105022-2), and the National Natural Science Foundation of China (40476053).

## References

- Adachi M, Sako Y, Ishida Y (1996) Analysis of *Alexandrium* (Dinophyceae) species using sequences of the 5.8S ribosomal DNA and internal transcribed spacer regions. *J Phycol* 32: 424–432
- Aguilera-Belmonte A, Inostroza I, Franco JM, Riobó P, Gómez PI (2011) The growth, toxicity and genetic characterization of seven strains of *Alexandrium catenella* (Whedon and Kofoid) Balech 1985 (Dinophyceae) isolated during the 2009 summer outbreak in southern Chile. *Harmful Algae* 12:105–112
- Alpermann T, Tillmann U, Beszteri B, Cembella A, John U (2010) Phenotypic variation and genotypic diversity in a planktonic population of the toxigenic marine dinoflagellate *Alexandrium tamarense* (Dinophyceae). *J Phycol* 46:18–32
- Alverson AJ, Kolnick L (2005) Intragenomic nucleotide polymorphism among small subunit (18S) rDNA paralogs in the diatom genus *Skeletonema* (Bacillariophyta). *J Phycol* 41:1248–1257
- Anderson D, Kulis D, Doucette G, Gallagher J, Balech E (1994) Biogeography of toxic dinoflagellates in the genus *Alexandrium* from the northeastern United States and Canada. *Mar Biol* 120: 467–478
- Anderson DM, Stock CA, Keafer BA, Bronzino Nelson A, Thompson B, McGillicuddy DJ, Keller M, Matrai PA, Martin J (2005) *Alexandrium fundyense* cyst dynamics in the Gulf of Maine. *Deep-Sea Res Pt II* 52:2522–2542
- Anderson DM, Alpermann TJ, Cembella AD, Collos Y, Masseret E, Montresor M (2012) The globally distributed genus *Alexandrium*: multifaceted roles in marine ecosystems and impacts on human health. *Harmful Algae* 14:10–35
- Baggesen C, Moestrup Ø, Daugbjerg N, Krock B, Cembella D, Madsen S (2012) Molecular phylogeny and toxin profiles of *Alexandrium tamarense* (Lebour) Balech (Dinophyceae) from the west coast of Greenland. *Harmful Algae* 19:108–116
- Bolch CJS, De Salas MF (2007) A review of the molecular evidence for ballast water introduction of the toxic dinoflagellates *Gymnodinium catenatum* and the *Alexandrium*. *Harmful Algae* 6:465–485
- Brosnahan ML, Kulis DM, Solow AR, Erdner DL, Percy L, Lewis J, Anderson DM (2010) Outbreeding lethality between toxic Group I and non toxic Group III *Alexandrium tamarense* spp. isolates: predominance of heterotypic encystment and implications for matting interactions and biogeography. *Deep-Sea Res Pt II* 57:175–189
- Burrell S, Gunnarsson T, Gunnarsson K, Clarke D, Turner AD (2012) First detection of paralytic shellfish poisoning (PSP) toxins in Icelandic mussels (*Mytilus edulis*): links to causative phytoplankton species. *Food Control*. <http://dx.doi.org/10.1016/j.foodcont.2012.10.002>
- Cembella AD (1998) Ecophysiology and metabolism of paralytic shellfish toxins in marine microalgae. In: Anderson DM, Cembella AD, Hallegraeff GM (eds) *Physiological ecology of harmful algal blooms*, NATO-Advanced Study Institute Series, vol 41. Springer, Heidelberg, pp 381–404
- Clark PU, Dyke AS, Shakun JD, Carlson AE, Clark J, Wohlfarth B, Mitrovica JX, Hostetler SW, McCabe AM (2009) The last glacial maximum. *Science* 325:710–714
- Coachman LK, Aagaard K (1966) On the water exchange through Bering Strait. *Limnol Oceanogr* 11:44–59
- Coleman AW (2007) Pan-eukaryote ITS2 homologies revealed by RNA secondary structure. *Nucleic Acids Res* 35:3322–3329
- Collins C, Graham J, Brown L, Bresnan E, Lacaze JP, Turrell E (2009) Identification and toxicity of *Alexandrium tamarense* (Dinophyceae) in Scottish waters. *J Phycol* 45:692–703
- Crespo BG, Keafer BA, Ralston DK, Lind H, Farber D, Anderson DM (2011) Dynamics of *Alexandrium fundyense* blooms and shellfish toxicity in the Nauset Marsh System of Cape Cod (Massachusetts, USA). *Harmful Algae* 12:26–38
- Edgar RC (2004) MUSCLE: multiple sequence alignment with high accuracy and high throughput. *Nucleic Acids Res* 32:1792–1797
- Fritz L, Triemer R (1985) A rapid simple technique utilizing calcofluor white M2R for the visualization of dinoflagellate thecal plates. *J Phycol* 21:662–664
- Ganley ARD, Kobayashi T (2007) Highly efficient concerted evolution in the ribosomal DNA repeats: total rDNA repeat variation revealed by whole-genome shotgun sequence data. *Genome Res* 17:184–191
- Genovesi B, Laabir M, Masseret E, Collos Y, Vaquer A, Grzebyk D (2009) Dormancy and germination features in resting cysts of *Alexandrium tamarense* species complex (Dinophyceae) can facilitate bloom formation in a shallow lagoon (Thau, southern France). *J Plankton Res* 31:1209–1224
- Gribble KE, Anderson DM (2007) High intraindividual, intraspecific, and interspecific variability in large-subunit ribosomal DNA in the heterotrophic dinoflagellates *Protoperdinium*, *Diplopsalis*, and *Preperidinium* (Dinophyceae). *Phycologia* 46:315–324
- Guillard RRL, Ryther JH (1962) Studies of marine planktonic diatoms. I. *Cyclotella nana* Hustedt and *Detonula confervacea* Cleve. *Can J Microbiol* 8:229–239
- Hoffert MI, Covey C (1992) Deriving global climate sensitivity from palaeoclimate reconstructions. *Nature* 360:573–576
- John U, Fensome RA, Medlin LK (2003) The application of a molecular clock based on molecular sequences and the fossil record to explain biogeographic distributions within the *Alexandrium tamarense* “species complex” (Dinophyceae). *Mol Biol Evol* 20:1015–1027

- Kim YO, Park MH, Han MS (2002) Role of cyst germination in the bloom initiation of *Alexandrium tamarense* (Dinophyceae) in Masan Bay, Korea. *Aquat Microb Ecol* 29:279–286
- Kim CJ, Yoshihiko S, Aritsune U, Kim CH (2004) Molecular phylogenetic relationships within the genus *Alexandrium* (Dinophyceae) based on the nuclear-encoded SSU and LSU rDNA D1–D2 sequences. *J Kor Soc Oceanogr* 39:172–185
- Lilly E, Kulis D, Gentien P, Anderson D (2002) Paralytic shellfish poisoning toxins in France linked to a human-introduced strain of *Alexandrium catenella* from the western Pacific: evidence from DNA and toxin analysis. *J Plankton Res* 24:443–452
- Lilly EL, Halanych KM, Anderson DM (2007) Species boundaries and global biogeography of the *Alexandrium tamarense* complex (Dinophyceae). *J Phycol* 43:1329–1338
- Macintyre J, Cullen J, Cembella A (1997) Vertical migration, nutrition and toxicity in the dinoflagellate *Alexandrium tamarense*. *Mar Ecol Prog Ser* 148:201–216
- Marret F, Zonneveld KAF (2003) Atlas of modern organic-walled dinoflagellate cyst distribution. *Rev Palaeobot Palynol* 125:1–200
- Medlin LK, Lange M, Wellbrock U, Donner G, Elbrächter M, Hummert C, Luckas B (1998) Sequence comparisons link toxic European isolates of *Alexandrium tamarense* from the Orkney Islands to toxic North American stocks. *Eur J Protistol* 34:329–335
- Miranda LN, Zhuang Y, Zhang H, Lin S (2012) Phylogenetic analysis guided by intragenomic SSU rDNA polymorphism refines classification of “*Alexandrium tamarense*” species complex. *Harmful Algae* 16:35–48
- Moestrup Ø, Hansen PJ (1988) On the occurrence of the potentially toxic dinoflagellates *Alexandrium tamarense* (= *Gonyaulax excavata*) and *A. ostenfeldii* in Danish and Faroese waters. *Ophelia* 28:195–213
- Montresor M, Lovejoy C, Orsini L, Procaccini G, Roy S (2003) Bipolar distribution of the cyst-forming dinoflagellate *Polarella glacialis*. *Polar Biol* 26:186–194
- Murata A, Nagashima Y, Taguchi S (2012) N:P ratios controlling the growth of the marine dinoflagellate *Alexandrium tamarense*: content and composition of paralytic shellfish poison. *Harmful Algae*. doi:10.1016/j.hal.2012.07.001
- Niemi A, Michel C, Hille K, Poulin M (2011) Protist assemblages in winter sea ice: setting the stage for the spring ice algal bloom. *Polar Biol* 34:1803–1807
- Oppen MJHV, Diekmann O, Wiencke C, Stam W, Olsen J (1994) Tracking dispersal routes phylogeography of the Arctic–Antarctic disjunct seaweed *Acrosiphonia arcta* (Chlorophyta). *J Phycol* 30:67–80
- Orlova TY, Selina MS, Lilly EL, Kulis DM, Anderson DM (2007) Morphogenetic and toxin composition variability of *Alexandrium tamarense* (Dinophyceae) from the east coast of Russia. *Phycologia* 46:534–548
- Orr RJS, Stüken A, Rundberget T, Eikrem W, Jakobsen KS (2011) Improved phylogenetic resolution of toxic and non-toxic *Alexandrium* strains using a concatenated rDNA approach. *Harmful Algae* 10:676–688
- Penna A, Garcés E, Vila M, Giacobbe MG, Fraga S, Luglié A, Bravo I, Bertozzini E, Vernesi C (2005) *Alexandrium catenella* (Dinophyceae), a toxic ribotype expanding in the NW Mediterranean Sea. *Mar Biol* 148:13–23
- Persich GR, Kulis DM, Lilly EL, Anderson DM, Garcia VMT (2006) Probable origin and toxin profile of *Alexandrium tamarense* (Lebour) Balech from southern Brazil. *Harmful Algae* 5:36–44
- Posada D (2008) jModelTest: phylogenetic model averaging. *Mol Biol Evol* 25:1253–1256
- Poulin M, Daugbjerg N, Gradinger R, Ilyash L, Ratkova T, von Quillfeldt C (2011) The pan-Arctic biodiversity of marine pelagic and sea-ice unicellular eukaryotes: a first-attempt assessment. *Mar Biodivers* 41:13–28
- Ratkova TN, Wassmann P (2005) Sea ice algae in the White and Barents seas: composition and origin. *Polar Res* 24:95–110
- Rodriguez F, Oliver J, Marin A, Medina JR (1990) The general stochastic model of nucleotide substitution. *J Theor Biol* 142:485–501
- Ronquist F, Huelsenbeck J (2003) MrBayes 3: Bayesian phylogenetic inference under mixed models. *Bioinformatics* 19:1572–1574
- Scholin CA, Anderson DM, Sogin ML (1993) Two distinct small-subunit ribosomal RNA genes in the North American toxic dinoflagellate *Alexandrium fundyense* (Dinophyceae). *J Phycol* 29:209–216
- Scholin CA, Herzog M, Sogin M, Anderson DM (1994) Identification of group- and strain-specific genetic markers for globally distributed *Alexandrium* (Dinophyceae). II. Sequence analysis of a fragment of the LSU rRNA gene. *J Phycol* 30:999–1011
- Scholin C, Hallegraeff G, Anderson D (1995) Molecular evolution of the *Alexandrium tamarense* ‘species complex’ (Dinophyceae): dispersal in the North American and West Pacific regions. *Phycologia* 34:472–485
- Sebastián CR, Etheridge SM, Cook PA, O’Ryan C, Pitcher GC (2005) Phylogenetic analysis of toxic *Alexandrium* (Dinophyceae) isolates from South Africa: implications for the global phylogeography of the *Alexandrium tamarense* species complex. *Phycologia* 44:49–60
- Tamura K, Peterson D, Peterson N, Stecher G, Nei M, Kumar S (2011) MEGA5: molecular evolutionary genetics analysis using maximum likelihood, evolutionary distance, and maximum parsimony methods. *Mol Biol Evol* 28:2731–2739
- Tang Y, Jiao Y, Zou E (2001) A Preliminary analysis of the hydrographic features and water masses in the Bering Sea and the Chukchi Sea. *Chin J Polar Res* 13:57–68 (in Chinese)
- Thornhill DJ, Lajeunesse TC, Santos SR (2007) Measuring rDNA diversity in eukaryotic microbial systems: how intragenomic variation, pseudogenes, and PCR artifacts confound biodiversity estimates. *Mol Ecol* 16:5326–5340
- Varela D, Paredes J, Alves-de-Souza C, Seguel M, Sfeir A, Frangópulos M (2012) Intraregional variation among *Alexandrium catenella* (Dinophyceae) strains from southern Chile: morphological, toxicological and genetic diversity. *Harmful Algae* 15:8–18
- Wang D, Hsieh DPH (2001) Dynamics of C2 toxin and chlorophyll-a formation in the dinoflagellate *Alexandrium tamarense* during large scale cultivation. *Toxicon* 39:1533–1536
- Weise AM, Levasseur M, Saucier FJ, Senneville S, Bonneau E, Roy S, Sauvé G, Michaud S, Fauchot J (2002) The link between precipitation, river runoff, and blooms of the toxic dinoflagellate *Alexandrium tamarense* in the St. Lawrence. *Can J Fish Aquat Sci* 59:464–473
- Woodgate RA, Aagaard K, Weingartner TJ (2005) Monthly temperature, salinity, and transport variability of the Bering Strait through flow. *Geophys Res Lett* 32:L04601. doi:10.1029/2004GL021880